Journal of Hydrology 525 (2015) 572–584

Contents lists available at ScienceDirect

Journal of Hydrology

journal homepage: www.elsevier.com/locate/jhydrol

Tree-ring based reconstruction of Río Bermejo streamflow in subtropical South America

María Eugenia Ferrero [a,*], Ricardo Villalba [a], Mónica De Membiela [a,b], Lidia Ferri Hidalgo [c], Brian Henry Luckman [d]

[a] Dendrocronología e Historia Ambiental, IANIGLA, CCT-CONICET-MENDOZA, CC 330, M5500 Mendoza, Argentina
[b] Universidad Politécnica de Madrid, Ciudad Universitaria s/n, 28040 Madrid, Spain
[c] Inventario Nacional de Glaciares, IANIGLA, CCT-CONICET-MENDOZA, CC 330, M5500 Mendoza, Argentina
[d] Department of Geography, University of Western Ontario, N6A 3K7 London, Canada

ARTICLE INFO

Article history:
Received 4 January 2015
Received in revised form 25 March 2015
Accepted 5 April 2015
Available online 9 April 2015

This manuscript was handled by Konstantine P. Georgakakos, Editor-in-Chief, with the assistance of David M. Meko, Associate Editor

Keywords:
Subtropical rivers
Northwestern Argentina
Tree-ring based reconstruction
South American Monsoon

SUMMARY

Precipitation on the subtropical Andes in northwestern Argentina is the main source of freshwater to rivers, which provide water for consumption, hydroelectric generation and irrigation of agricultural fields. Regional streamflow records for the past 60 years indicate a period of enhanced inter-annual and inter-decadal variability during recent decades. Here we present a long-term perspective of streamflow variations for Río Bermejo, a major river in the subtropics of Argentina–Bolivia. This streamflow reconstruction covers the period 1680–2001 and was performed using principal component regression models based on precipitation sensitive tree-ring width series. Composite tree-ring chronologies from *Juglans australis*, *Cedrela lilloi* and *Schinopsis lorentzii* were used as predictors to reconstruct the May–October (dry season) streamflow variations. Monthly instrumental streamflow records were used to assess the temporal relationship between climatic data and tree-ring records. The regression model explains 52% of the variance of May–October Bermejo discharge (R^2 *adj* = 0.499) over the period 1941–1992. Analyses of the frequency, intensity and duration of pluvials and droughts indicates a sustained increase in streamflow since the 1960s, which is exceptional since 1680. Pearson's correlation coefficients between Río Bermejo records against gridded interpolated precipitation and outgoing longwave radiation indicate that the South American monsoon is the main source of regional precipitation and the consequent discharge of subtropical rivers in northern Argentina. Long-term streamflow reconstructions in subtropical South America contribute to our understanding of past and present climate variations and the related large-scale atmospheric features that drive these variations.

1. Introduction

Water scarcity is a major constraint for the socio-economic development of a region. Water shortages severely impact food production, electric power generation and access to clean drinking water (Arnell et al., 2001; Viviroli et al., 2003). Hence, the management of water resources requires a comprehensive view of their natural variability over multiple time scales (Woodhouse and Lukas, 2006). Long-term records are vital to provide reliable patterns of runoff variability from interannual to decadal and longer scales. However, in tropical and subtropical South America long and high quality meteorological and hydrological records are rare and few records exceed 50 years in length. Although these gauge records are used for planning and engineering design of irrigation and hydropower infrastructures, they are too short to determine the true discharge variability, particularly the severity and duration of high (pluvial) and low flow (drought) periods in subtropical South America.

Water resources from mountainous regions are vital to natural ecosystems and human activities in the adjacent lowlands. This is particularly the case in arid and semiarid regions of the world, where water from mountains contributes between 50% and 90% of total streamflow (Messerli et al., 2004). Detailed assessments of the main hydrological patterns and factors affecting mountain hydrology conditions are still limited in many regions, despite the importance of mountains as sources of freshwater (Masiokas et al., 2013). Río Bermejo basin covers over 123,000 km^2 in the

* Corresponding author at: Av. Ruiz Leal s/n, Parque San Martín, CC 330, CP M5500 Mendoza, Argentina. Tel.: +54 261 5244203; fax: +54 261 5244200.
E-mail addresses: mferrero@mendoza-conicet.gob.ar (M.E. Ferrero), ricardo@mendoza-conicet.gob.ar (R. Villalba), monicademembiela@yahoo.es (M. De Membiela), lferri@mendoza-conicet.gob.ar (L. Ferri Hidalgo), luckman@uwo.ca (B.H. Luckman).

http://dx.doi.org/10.1016/j.jhydrol.2015.04.004
0022-1694/

tropical and subtropical sectors of southern Bolivia and northwestern Argentina. Starting from the high Andes in northwest Argentina and southwest Bolivia, Río Bermejo flows eastwards over 1,300 km to contribute to the Paraguay-Paraná river system (Rafaelli et al., 2001). Total basin population is estimated as ca. 1.3 million (COBINABE, 2010), of which 39% is located in semi-urban/rural sectors (small cities, rural farmers and indigenous communities) (Manzanal and Arrieta, 2000). Livestock breeding, which is an important source of income for rural populations, is mainly concentrated in flood pasture lands where cattle are reared wildly, taking advantage of natural watering places during the dry season.

Sediment concentrations in Río Bermejo average 8 kg/m^3, amongst the highest in the world and the river discharges ca. 100 million tons/year to Río Paraguay. Although Río Bermejo contributes only 2% of total discharge it provides almost 50% of the total suspended solid material delivered to Río de la Plata (Pedrozo and Bonetto, 1987; Brea and Spalletti, 2010), the second largest river in South America after the Amazon. Most of the suspended sediment originates from erosion of unconsolidated deposits during the rainy season in the basins of Río Iruya and Río Grande (upper Río Bermejo basin; Rafaelli et al., 2001). As a result of the large amount of sediment transport, the river periodically changes its course in the lower and flatter sectors of the basin. Consequently, this dynamic behavior has hampered the effective use of water for irrigation in the lower part of the basin. Argentina and Bolivia established a Binational Commission (COBINABE, Comisión Binacional de los ríos Bermejo y Grande de Tarija) for the sustainable natural resource management in both watersheds. In 1995, this Binational Commission requested assistance from the World Bank, through the Global Environmental Facility (FMAM/GEF) to develop a water resource management program for the Río Bermejo-Grande de Tarija basins. The GEF assistance proposed a Strategic Action Program that could solve the trans-boundary environmental problems affecting the basins. Clearing of forests for cultivation and widespread overgrazing has accelerated biodiversity loss, erosion, water scarcity, floods and other environmental hazards (Gasparri et al., 2013). Forest loss and cattle ranching also aggravate sediment mobilization contributing to downstream environmental degradation and reducing the quality of life and cultural resources of native population (OAS, 2005). Moreover, a drier or longer dry season also places considerable stress on communities without access to reliable municipal or groundwater sources (Anchukaitis et al., 2014). In this context, a better understanding of Río Bermejo interannual fluctuations is critical to assess streamflow variability at different temporal scales (Woodhouse and Lukas, 2006; Urrutia et al., 2011).

Tree rings provide annually-resolved records which can be used as proxy for reconstructing long-term variability in regional hydroclimate (Meko and Woodhouse, 2011). Tree growth is influenced by the same climatic variables that modulate runoff, particularly precipitation and evapotranspiration. Therefore annual or seasonal variations in discharge may be reconstructed from tree rings based on the strong relationship between tree-growth and river discharge. A number of tree-ring based streamflow reconstructions has been developed for North America (see Meko and Woodhouse, 2011 and references therein). However, only seven reconstructions have been developed in South America, four in Chile (Lara et al., 2008; Urrutia et al., 2011; Muñoz, 2012; Lara et al., 2014) and three in Argentina (Holmes et al., 1979; Cobos and Boninsegna, 1983; Mundo et al. 2012). In Argentina, the first streamflow reconstruction was developed by Holmes et al. (1979) who extended the Río Limay and Río Neuquén records back to 1601 using *Araucaria araucana* and *Austrocedrus chilensis* tree-ring chronologies from northern Patagonia. Cobos and Boninsegna (1983) used *Austrocedrus* tree rings from central Chile to reconstruct the streamflow for the Atuel River in Argentina back to 1576. Recently, Mundo et al. (2012) updated and extended the reconstruction of Río Neuquén over the period 1346–2000.

Tree-ring based reconstructions of hydrological and climatic variations in tropical and subtropical regions of South America are rare, reflecting the paucity of tree-ring chronologies in these regions. In tropical South America, temporal variation in the Amazon River discharge has been inferred from a single chronology of *Piranhea trifoliata* growing in seasonally-flooded plains (Schöngart et al., 2004). In the subtropics, Flamenco et al. (2011) developed a preliminary flow reconstruction of Río San Francisco, a tributary of Río Bermejo utilizing artificial neural network structures drawn from two ring-width chronologies (*Juglans australis* and *Cedrela lilloi*).

In this study we develop a multi-century tree-ring based reconstruction for Río Bermejo streamflow using a nested multiple regression approach (Meko, 1997; Cook et al., 2002). This is the first statistically validated hydrological reconstruction for the subtropics and uses a network of subtropical chronologies in nortwestern Argentina. We also identify the dominant oscillatory modes in the Río Bermejo streamflow reconstruction and their relationships with regional and continental atmospheric circulation.

2. Study area

2.1. Regional climate

The South America Summer Monsoon (SASM) is induced by low-latitude temperature differences between the continent and the oceans and modulates the atmospheric circulation over tropical-subtropical South America in summer (IPCC, 2007; Garreaud et al., 2009). The onset of the wet season in central and southeastern Amazonia typically occurs between the end of September and early October and by late November deep convection covers most of the central South America from the equator to 20°S. During the mature phase of SASM between late November and late February, the area of main convective activity is centered over tropical central South America and connects with a convection band of cloudiness and precipitation extending from southern Amazonia toward southeastern Brazil and the adjacent Atlantic Ocean (Vera et al., 2006). This diagonal band of precipitation maxima over the ocean is known as the South Atlantic Convergence Zone (SACZ). The SACZ is evident year round but more intense during summer, producing episodes of intense rainfall over much of southeastern South America. At intraseasonal timescales, the SACZ is part of a see-saw pattern of precipitation over eastern South America. Periods of enhanced precipitation over the SACZ are accompanied by decreased rainfall in subtropical plains of northern Argentina, Paraguay and Uruguay, including the Río Bermejo basin. Opposite, roughly symmetric conditions prevail during weak SACZ periods. As a regional response to the strong convective heating over the Amazon, an upper-level high-pressure cell, called the Bolivian High, is formed. At low levels, a deep continental low is formed over the Chaco region (the Chaco Low). The interaction between circulation associated with the Chaco Low and the Andes reinforces the transport of moisture from tropical to subtropical South America. The regional intensification of the air circulation east of the Andes is due to the South American Low-Level Jet (SALLJ) which transports considerable moisture between the Amazon and La Plata basin over the subtropical plains as far as 35°S (Paegle and Mo, 2002; Saulo et al., 2004). In northwestern Argentina, humid air masses moving from northeastern to southwestern collide with the mountain ranges, forcing the air to rise and cool generating abundant orographic precipitation.

2.2. Río Bermejo basin

The Bermejo basin covers 11,896 km^2 in southern Bolivia and 111.266 km^2 in northern Argentina (Fig. 1). It is the largest basin in northwestern Argentina with the third largest discharge. The basin encompasses three different topographic environments: the upper-elevation Puna plateau, the sub-Andean mountains and the Chaco plains with contrasting climatic conditions as reflected in regional vegetation (Cabrera, 1976; Pedrozo and Bonetto, 1987). Subtropical montane deserts at high elevations give way to humid forests in the mountain valleys and dry forests in the extensive lowlands. Most runoff of Río Bermejo is generated from the humid slopes of the Andes which receive the greatest precipitation. Over short distances the climates change from semiarid montane cold climates to the west (Prepuna) to seasonally wet intermountain valleys (sub-Andean mountains) ending in topical warm-dry forests in eastern lowland area (Chaco plains).

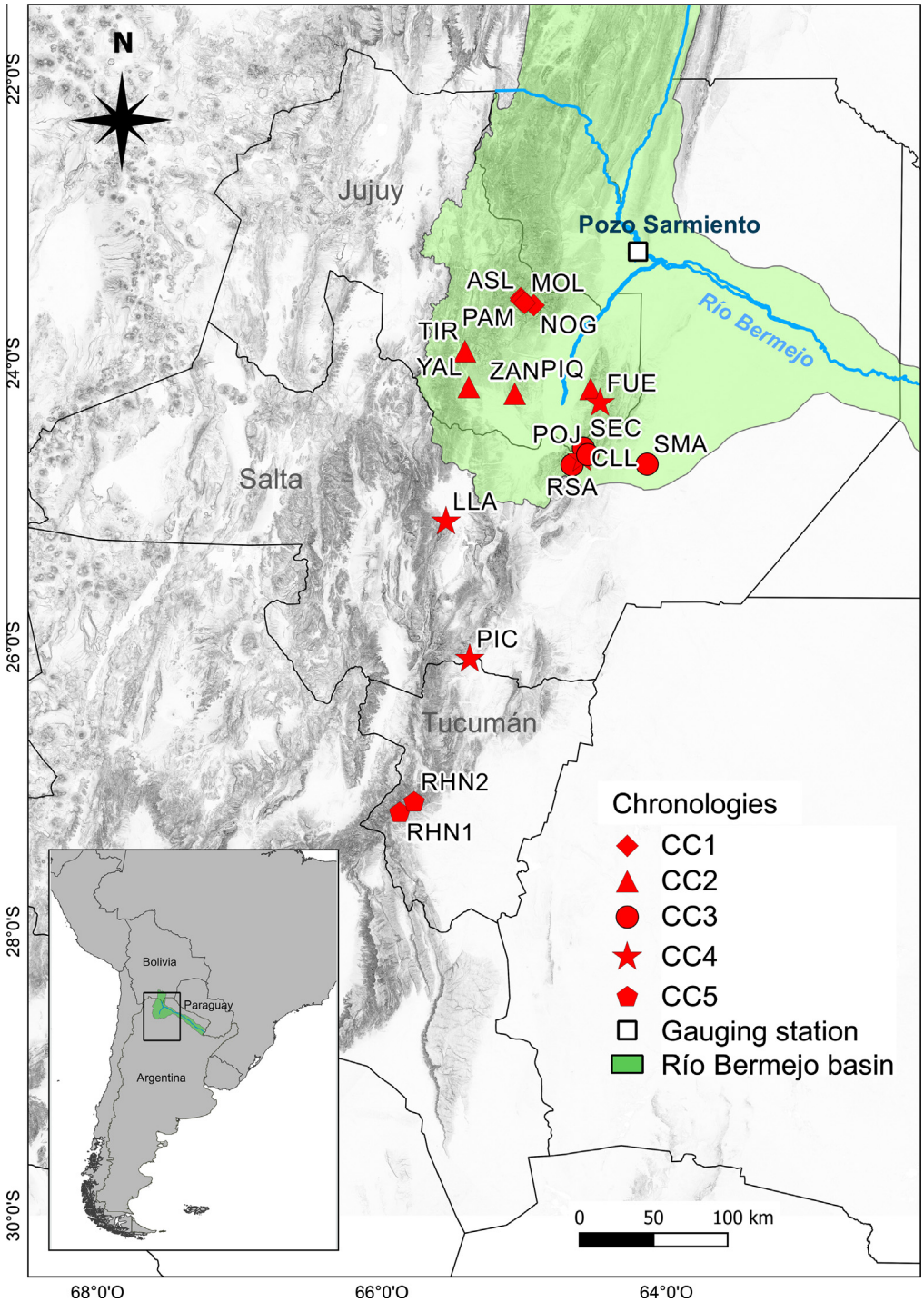

Fig. 1. Map of subtropical northwestern Argentina showing the Bermejo basin (shaded light-green area), the location of Pozo Sarmiento gauging station (white square) and tree-ring chronologies used in this study. Each symbol represent a single chronology location; tree-ring chronologies with identical symbols were grouped to produce the composite chronologies "CC" (for reference, see Table 1). (For interpretation of the references to colour in this figure legend, the reader is referred to the web version of this article.)

3. Material and methods

3.1. Streamflow data

The hydrological regimes of rivers in the region are distinctly monsoonal with a well-defined unimodal seasonality exhibiting 75–85% of flows in the rainy summer season (January–April) and only ca 11% in the dry winter season (May–September) (Pedrozo and Bonetto, 1987; Brea and Spalletti, 2010). Heavy rains in the Sierras Subandinas are responsible for major floods and avulsions in the middle and lower basin, causing considerable damage to agricultural fields and livestock production, cutting roads and isolating rural populations.

This seasonality results in strong extremes in Río Bermejo streamflow with minimum-recorded flows of 20 m^3/s and maxima greater than 12,000 m^3/s. The Subsecretaría de Recursos Hídricos de la Nación (SSRH, National Agency of Water Resources of Argentina) operates many gauging stations in the Río Bermejo basin. The Pozo Sarmiento gauge station (23°13′S, 64°12′W; 296 m, drainage area 25,000 km^2) has one of the longest (1940–2013) and most complete records and has generally been used as a reference for the behavior of the upper basin. The mean annual discharge at Pozo Sarmiento is 4,512 m^3/s, with peak flows up to 11,260 m^3/s. The hydrological year runs from September to August of the following year (Fig. 2).

3.2. Northwestern Argentina tree-ring chronologies

The complex topography of northwestern Argentina results in a variety of montane and lowland habitats, which is reflected in the wide range of woody species with potential for dendrochronological studies (Ferrero et al., 2014). However, previous studies show that many of these species have high growth rates and, although they can reach large diameters, they rarely exceed 100 years of age. The hardness of the wood in most long-lived species prevents sampling with traditional increment borers and therefore sampling of those species is limited to sites with forest harvesting.

The first dendrochronological records in the subtropical regions of Argentina were developed from *J. australis* and *C. lilloi* in the 1980s (Villalba et al., 1987,1992). Many of these records were recently updated and new chronologies developed from other subtropical species such as *Schinopsis lorentzii* (Ferrero and Villalba, 2009; Ferrero et al., 2013). Currently we have an extended network of chronologies available from the subtropical montane forests of northwestern Argentina (Boninsegna et al., 2009) that can potentially be used to develop reconstructions of river flows in subtropical areas of South America.

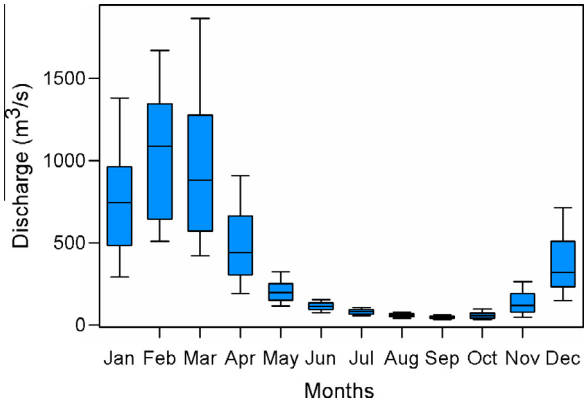

Fig. 2. Mean monthly hydrograph (with minimun and maximun values -*caps*-) of Río Bermejo estimated over the period 1941–2012 at Pozo Sarmiento gauge station. December (of previous year) to April discharge accounts for 85% of the total annual flow.

In Argentina *J. australis* (Juglandaceae) and *C. lilloi* (Meliaceae) are present in a narrow belt (22°–29°S, 64°–66°W) along the Sierras Subandinas, representing the southernmost extension of the tropical cloudy forests in South America (Brown et al., 1985; Grau and Brown, 1995). *J. australis* grows between 650 and 2500 m and *C. lilloi* between 1100 and 2500 m (Cabrera, 1976). *S. lorentzii* (Anacardiaceae) grows at altitudes below 500 m in southeastern Bolivia and Paraguay, and on the sub-Andean slopes of northwestern Argentina (64°–60°W; Cabrera, 1976; Spichiger et al., 1995).

Hydrological regimes of most rivers in subtropical South America are largely regulated by regional rainfall patterns. Previous studies showed that tree growth in northwestern Argentinean forests is mostly influenced by precipitation and to a lesser extent by temperature variations (Villalba et al., 1992; Ferrero, 2011; Ferrero et al., 2013). A principal component analysis (PCA) of the tree-ring chronology network showed that the first principal component, which explains 26% of the total variability in the chronologies, is strongly connected with precipitation variations in subtropical northwestern Argentina (Ferrero, 2011).

3.3. Chronology development

Ring-width chronologies used in this study cover a substantial variety of environments (Fig. 1 and Table 1). Cores from living trees were collected from 32 sites (27 *J. australis*, 4 *C. lilloi*, 1 *S. lorentzii*). At each of the 32 sampled sites, at least two cores from 10 to 39 trees were collected using increment borers. Cores were sanded and tree rings measured to 0.001 mm precision. Series were cross-dated visually and subsequently verified using the computer program COFECHA (Holmes, 1983). Radii from nearby sites and/or with high correlation due to similarities in environmental conditions, were grouped to construct composite chronologies. The final selection of individual tree-ring series entering in the composite chronologies was conducted using the program COFECHA (Holmes, 1983), setting a minimum correlation of $r = 0.32$ for each series with the master chronology. This procedure significantly increased replication, integrate regional environmental variations and enhanced the common signal and chronology quality.

Tree-ring series were standardized and averaged to produced eight composite chronologies. Standardization of the individual tree-ring series minimizes the variability in the tree-ring series not related to climate (age trends and local disturbances; Fritts, 1976). Several standardization trials were carried out using the program ARSTAN 40 (Cook and Krusic, 2005). Standard composite chronologies were standardized using negative exponential curves or linear regression with negative or zero slope. The process reflect interannual variations in tree growth but preserves a large portion of the low-frequency variation. The variance of the chronologies over time was stabilized using the method described by Osborn et al. (1997).

The quality of the composite tree-ring chronologies was evaluated estimating the mean correlation between all series (RBAR) and expressed population signal (EPS, Table 1). The RBAR is a measure of the common variance between all series in a chronology (Wigley et al., 1984), whereas the EPS is a measure of the similarity between a chronology and a hypothetical chronology that has been infinitely replicated (Briffa, 1995). When the EPS value for a segment (50 or more years) in a chronology is above a determined threshold (0.85), the chronology segment is considered robust reflecting temporal stability, good quality, and a strong common signal between samples in this particular segment (Wigley et al., 1984). The EPS statistic is particularly sensitive to the chronology

Table 1
Tree-ring chronologies (left panel) and species selected to produce the composite chronologies; descriptive statistics of final composite chronologies (right panel) used as potential predictors for Río Bermejo streamflow variations in northwestern Argentina. Chronologies used in the final nested reconstruction are shown in bold.

Tree-ring chronologies					Composite chronologies[a]						
Site	Chronology	Latitude, Longitude	Elevation (m)	Composite chronology (CC) code	Period AD	Cores	Series intercorrelation	AMS	RBAR	EPS[b]	Corr. coeff. with May–Oct Bermejo river streamflow[c]
Cedrela lilloi											
LMC	La Mesada	22°36′S, 64°37′W	1600		1752–2002	164	0.442	0.437	0.305	0.947 (1796)	
LTC	Los Toldos	22°19′S, 64°37′W	2700								
TOC	Los Toldos	23°11′S, 64°25′W	2025								
REC	Cerro Chañar	24°26′S, 64°35′W	1700								
Juglans australis											
LMJ	La Mesada	23°12′S, 64°37′W	1460		1709–1999	127	0.445	0.422	0.277	0.932 (1766)	
TON	Los Toldos	22°11′S, 64°18′W	1875								
VAL	Vallecito	22°14′S, 64°48′W	1880								
SJJ	San José	23°38′S, 64°33′W	980								
ARR	Arrasayal	22°26′S, 64°19′W	880								
RPJ	Río Pescado	22°42′S, 64°33′W	1200								
NOG	**Nogalar**	**23°35S, 64°55W**	**1840**	**CC1**	**1779–2006**	**194**	**0.577**	**0.468**	**0.346**	**0.938 (1812)**	**0.426** (***t*–*1***)
PAM	**Pampichuela**	**23°32S, 65°01W**	**1843**								
ASL	**A San Lucas**	**23°33S, 65°01W**	**1680**								
MOL	**Molular**	**23°34S, 64°59W**	**1881**								
TIR	**Tiraxi**	**23°55S, 65°25W**	**1900**	**CC2**	**1678–2003**	**123**	**0.465**	**0.445**	**0.325**	**0.910 (1734)**	**−0.615** (***t***) **−0.431** (***t*** **− 1**) **−0.372** (***t*** **− 2**) **−0.490** (***t*** **+ 1**)
YAL	**Yala**	**24°10S, 65°23W**	**1660**								
ZAN	**Zapla**	**24°13S, 65°04W**	**1893**								
PIQ	**Piquete**	**24°11S, 64°32W**	**1900**								
FUE	**El Fuerte**	**24°17S, 64°28W**	**1295**	**CC4**	**1789–2004**	**122**	**0.444**	**0.366**	**0.200**	**0.923 (1794)**	**0.406** (***t*–1**)
CLL	**Cascada Los Lobitos**	**24°40S, 64°35W**	**909**								
LLA	**Los Laureles**	**25°07S, 65°32W**	**1650**								
PIC	**Arroyo Pichanas**	**26°05S, 35°23W**	**1070**								
CAJ	El Cajón	26°27′S, 64°54′W	854		1813–2004	82	0.489	0.491	0.339	0.933 (1882)	
NIO	Río Nío	27°16′S, 64°34′W	1300								
ESC	Dique Escaba	27°25′S, 65°27′W	900								
LAJ	Las Lajas	27°48′S, 65°43′W	1182								
RHN1	**Río Horqueta**	**27°10S, 65°53W**	**1850**	**CC5**	**1680–1992**	**65**	**0.610**	**0.382**	**0.538**	**0.926 (1682)**	**−0.516** (***t***) **−0.421** (***t*** −1) **−0.505** (***t*** −2)
RHN2	**Río Horqueta**	**27°10S, 65°52W**	**1740**								
Juglans australis+Schinopsis lorentzii (SMA)											
SEC	**Senda del Ciervo**	**24°36S, 64°35W**	**900**	**CC3**	**1820–2001**	**87**	**0.440**	**0.483**	**0.287**	**0.933 (1854)**	**0.455** (***t***) **0.394** (***t*** −2)
POJ	**Popayán**	**24°38S, 64°33W**	**700**								
RSA	**Río Sala**	**24°43S, 64°39W**	**700**								
SMA	**San Martín**	**24°42S, 64°08W**	**458**								

[a] Descriptive statistics for composite chronologies. AMS, average mean sensitivity; RBAR, mean correlation between series; EPS, average expressed population signal.
[b] Mean expressed population signal; the year at which each chronology reaches the 0.85 threshold, is given in parentheses.
[c] Corr. Coeff. with May–Oct Bermejo river streamflow; significant correlations between composite tree-ring chronologies and May–October Bermejo streamflow over the 1940–2005 period for lags $t = 0$, $t - 1$, $t - 2$ and $t + 1$ ($P < 0.01$); only correlations of the records finally included in model are shown.

replication and points out the minimum number of samples in a chronology required to maintain a strong common signal.

3.4. Streamflow reconstruction

We computed correlation coefficients between the composite chronologies and instrumental Río Bermejo records to establish the relationships between tree growth and river discharge. All tree-ring chronologies were compared with streamflow at year $t = 0$, and lagged at years $t - 2$, $t - 1$ and $t + 1$ to account for tree-growth preconditioning and delayed responses to climate, two features common in tree-ring series (Fritts, 1976). All chronologies were compared with various monthly and seasonal combinations of Río Bermejo streamflow, following the methods described by Fritts (1976) and Blasing et al. (1984). The strongest relationships occurs when tree-ring composite chronologies are compared with seasonal flows from May to October (6-month period). This is the period of lowest annual streamflow in Río Bermejo (Fig. 2) and consequently, the most suitable to reveal regional droughts. Only those composite chronologies showing correlations $r \geqslant \pm 0.40$ ($P < 0.01$) with streamflows were selected for further analysis (Table 1). The occurrence of close relationships between tree-ring records and runoff during the dry period of the year has already been reported for other species growing in environments with marked seasonality in rainfall (Lara et al., 2008). These relationships seem to indicate that the radial growth of trees is more sensitive to the low rainfalls during the dry period than to the excess of water in the soil during the monsoonal wet period.

Since the shortest record in the set of predictors limits the length of the reconstruction, a nested principal component regression (PCR) approach was used to maximize the length of the available records (Meko, 1997; Cook et al., 1999, 2002). The composite tree-ring series significantly correlated with May–Oct dry season streamflow (Table 1) were entered into a principal component analysis to reduce the number of predictors and enhance the common signal (Cooley and Lhones, 1971). Following the Kaiser-Guttman rule those PCs with eigenvectors > 1.0 were retained in the stepwise multiple regression. The selection criterion for the final regression model was to maximize the adjusted R^2. Following this method, five reconstructions, based on different sets of increasingly longer tree-ring composite series, were produced. The shortest predictor series (i.e. the composite tree-ring chronology covering the shortest time interval) was progressively excluded from the regression analyses, and the regression procedure repeated again utilizing the remaining, longer chronologies (Cook et al., 2004).

Each reconstruction was based on the largest common period between predictors and predictans (1941–1992 or 1941–2001) and was developed using a "leave-one-out" cross-validation procedure (Michaelsen, 1987). Linear regression models for each year were successively calibrated on the remaining 50 (59) years and then used to estimate the observed streamflow value for the year omitted at each step. This resulted in 51 (60) estimated streamflow values which were compared to the actual streamflow observations to compute validation statistics of model accuracy and error. Regression models based on the full calibration dataset (1941–1992 or 1941–2001) were used to reconstruct the streamflow.

The goodness of fit between observed and predicted streamflow values was tested based on the proportion of variance explained by the regression in combination with the normality, and first-order autocorrelation of the regression residuals (Table 2). As an additional measure of regression accuracy, we also computed the Reduction of Error (RE) statistic (Fritts, 1976; Cook et al., 1994). The root mean square error of validation (RMSEv) (Weisberg, 1985) was calculated and used as an estimate of the uncertainties of the reconstructions. To derive the final reconstruction, we spliced together the relevant segments from each nested model. The mean and variance of each nested reconstruction was adjusted to the most replicated nest in order to minimize artifact-related changes in variance though time (e.g. Cook et al., 2004; D'Arrigo et al., 2011).

3.5. Spectral properties of the reconstruction

Intensity and distribution of low and high flows (<10th and >90th percentiles, respectively) in the Bermejo river were examined over the reconstructed period. The Blackman–Tukey (BT) power spectra was used to assess the oscillatory domains in the Río Bermejo reconstruction over the 1680–2001 period. In this analysis, the BT spectrum was estimated from 97 lags of autocorrelations (30% of the series length), which provides a reasonable balance between high resolution and moderate stability. The 95% confidence level of the spectrum was estimated from a "red noise" first-order Markov null continuum based on the lag-1 autocorrelation of the time series (Mitchell et al., 1966). Coherence and singular spectral analyses were used to depict the temporal evolution of the dominant periods in the river reconstruction and in the instrumental records. Coherence analysis (Jenkins and Watts, 1968) measures the common variance as a function of frequency between the instrumental and reconstructed records, while singular spectral analysis (SSA, Vautard and Ghil, 1989) is a statistical technique related to empirical orthogonal functions that was used to detect and extract the main oscillatory modes of both instrumental and reconstructed series over time.

3.6. Links between streamflow and atmospheric circulation anomalies

We utilized the spatial correlation patterns between reconstructed and instrumental streamflow records and several meteorological variables across South America and surrounding oceans to identify the atmospheric-oceanic forcings that modulate interannual to multi-decadal scale variations in Río Bermejo discharge.

Outgoing longwave radiation (OLR) (Liebmann and Smith, 1996) is commonly used as a proxy for precipitation in the tropics and used as an index of deep tropical convection; low values indicate major convective systems with high and cold cloud tops and are associated with rainfall and latent heat release (Camilloni

Table 2
Calibration and verification statistics for the five nested reconstruction models.

Model (period covered by predictors AD)	Predictors	Adj R^2 (F)	*Se*	*RE*	DW*d*	RMSEv
1 (1821–1992)	All composite tree-ring chronologies	0.499 (17.23)	103.941	0.41	1.85	110.097
2 (1788–1992)	All composite except CC3	0.493 (24.77)	104.541	0.43	1.93	108.911
3 (1778–1992)	All composite except CC3 and CC4	0.492 (24.65)	104.674	0.43	1.88	108.959
4 (1680–1992)	Only CC5 composite chronology	0.290 (20.43)	123.658	0.23	1.32	126.025
5 (1821–2001)	CC1, CC2 and CC3 composite chronologies	0.279 (11.92)	129.645	0.21	1.51	133.452

Models were cross-validated using a leave-one-out approach (see text).
Adj R^2, coefficient of determination adjusted to account for the number of predictors in each model, used as an indicator of the proportion of variance explained by regression; *F*, *F*-value of regression; *Se*, standard error of estimate; *RE*, reduction of error estimate; DWd, Durbin–Watson *d* statistics used to test the first-order autocorrelation of the regression residuals; RMSEv, root mean squared error of validation.

and Barros, 2000). Pearson's correlation coefficients between the instrumental streamflow and spatial variations of OLR were estimated over the South American continent. We also estimated the spatial relationships between the reconstructed streamflow and total monthly precipitation using data from the University of Delaware gridded (0.5 × 0.5) dataset. The NCEP-NOAA (http://www.cdc.noaa.gov/correlation) reanalysis data were also used to build the spatial correlation patterns.

4. Results

4.1. Río Bermejo streamflow reconstruction

The final reconstruction of May–October dry season Río Bermejo (Fig. 3) streamflow was based on 5 nested regression models (Table 2), accounting for (R^2 adjusted for loss of degrees-of-freedom): 29% (1680–1777), 49% (1778–1787), 49% (1788–1820), 50% (1821–1992) and 28% (1993–2001) of the instrumental river discharge variability during the calibration periods (1941–1992/1941–2001). Since the standard error of the estimate *Se* is a measure of the accuracy (dispersion) of predicted scores in a regression, the lower skill of the less replicated regression models (1680–1777 and 1993–2001) are consistent with the highest values of *Se* (Table 2).

According to Durbin–Watson tests, the residuals of the regression models are not significantly autocorrelated. Nevertheless, the skill of the regression model for the earliest part of the reconstruction was rather poor compared to models based on a larger number of predictors. Despite these limitations all models, including the less-replicated Models 4 and 5 (Table 2) successfully passed

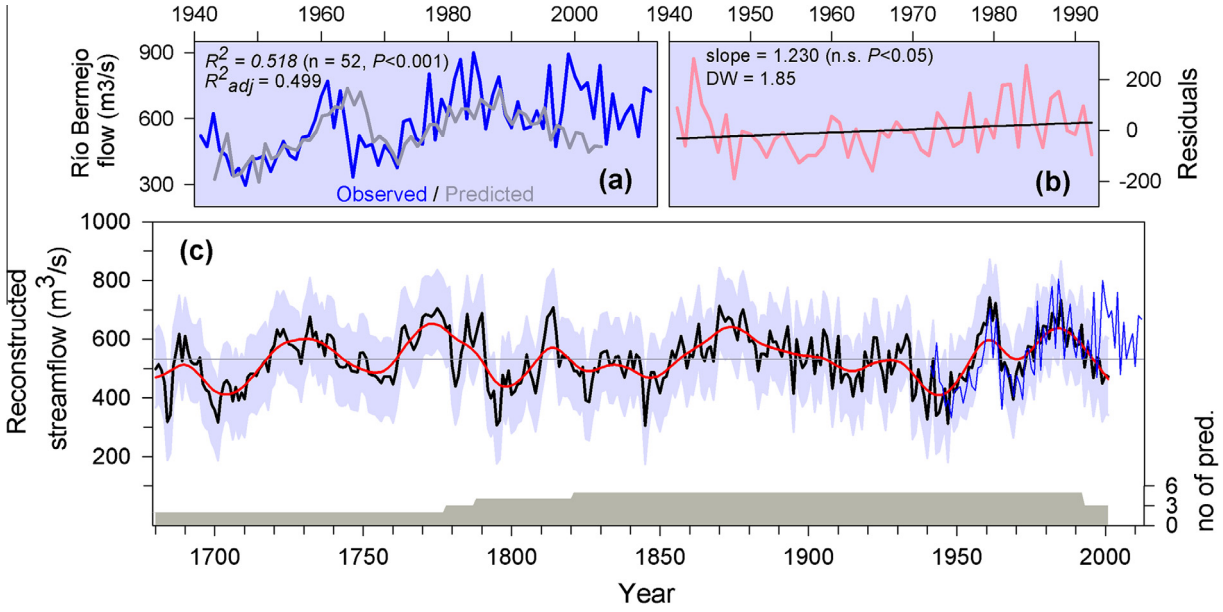

Fig. 3. Reconstruction of May–October Río Bermejo streamflow variations. (a) Instrumental (blue) and tree-ring based reconstruction (grey) for the 1941–2012 period. Coefficient of determination (an indicator of the proportion of variance explained by regression) (R^2) and adjusted by degrees of freedom in the model (R^2_{adj}) show statistically significant positive correlations between tree-ring and instrumental streamflow variations. (b) Regression residuals (red) for the reconstruction with linear trend (slope; black line) and the Durbin–Watson (DW) *d* statistics used to test for first-order autocorrelation of regression residuals are also indicated. (c) Nested tree-ring based reconstruction of May–October river streamflow variations over the period 1680–2001. Shaded areas denotes the 1 ± root-mean-square error, which estimates the uncertainty of the reconstructed series. To emphasize the low-frequency variations, a 25-yr smoothing cubic spline designed to reduce 50% of the variance is shown in red. Blue line represents the 1941–2012 instrumental record. (For interpretation of the references to colour in this figure legend, the reader is referred to the web version of this article.)

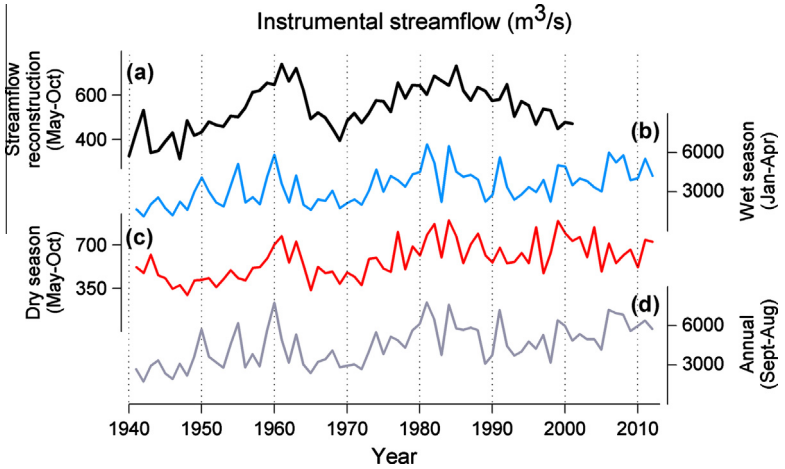

Fig. 4. Reconstructed streamflow from tree-ring series of northwestern Argentina (a) compared with temporal variations of the Río Bermejo discharge for the 1941–2012 period (data from Pozo Sarmiento gauge station): (b) Bermejo river discharge corresponding to the wet season (from January to April), $r = 0.506^*$; (c) the same as (b) but for the dry season (May to October), $r = 0.720^*$; (d) annual discharge for the hydrological year of the Bermejo river (from September to August), $r = 0.497^*$. *All correlations given (with the most replicated portion of the reconstruction – up to 1992) are statistically significant at $P < 0.01$ ($n = 52$).

the verification process (positive *RE and significant RMSEv*), which implies highly significant predictive skill of subtropical tree-ring chronologies to infer past changes in Río Bermejo streamflow.

As previously indicated, the composite tree-ring chronologies used to reconstruct Río Bermejo streamflow are more strongly related to the river discharge during the dry period. Nevertheless, statistically significant correlations also occur when the tree-ring based reconstruction for the dry period is compared with total annual or summer discharges (Fig. 4). Baseflow discharge during the dry months is significantly correlated with the streamflow during the wet period (Dec–Apr, $r = 0.356$; $P < 0.001$), suggesting a persistence effect of wet season precipitation in both streamflow and tree growth during the following dry season.

The Río Bermejo reconstruction showed important interannual to multidecadal variability over the past 321 years (Fig. 3). An increase in streamflow variability is registered from ~1780 to 1810 and more recently from ~1940 to 1970 with a large peak centered on 1950. The Río Bermejo reconstruction suggests an increase in the recurrence of extreme wet events during the twentieth century. The reconstruction does not show the occurrence of a wet period as extensive as that recorded in the last few decades. Wet events "pluvials" are generally less extreme than those observed during the period of calibration. The most important humid periods identified in the reconstruction occurred around 1770–80, 1870–80 and from early 1960 to the present (Fig. 5). The years of greatest flow (above the 98th percentile in the whole reconstruction) are more frequent in the last four decades. Three of the five years with most extreme flows (1814, 1870, 1961, 1963, 1985) occurred after 1961. Similarly, even though reconstructed dry events are more evenly distributed within the series, three of the seven driest years (below 2nd percentile) are in the 1940s (1701, 1795, 1796, 1845, 1940, 1943, 1947).

Coherence spectral analysis indicated that Río Bermejo reconstruction captures some interannual to decadal variability over the instrumental period, with significant values of squared coherency between 9 and 15 years (Fig. 6a). The Blackman–Tukey spectrum of the reconstructed Bermejo streamflow, which shows the distribution of variance as a function of frequency, reveal important peaks at 48.5, 27.7, 13.9, 7.2 and 2.9 years (Fig. 6b). Consistent with the Blackman–Tukey spectrum, the SSA analysis of the reconstruction identifies six dominant waveforms, with oscillatory modes at 109, 47, 25, 14 and 8 years (Figs. 7a–e, respectively). Applying SSA to the instrumental streamflow records, dominant oscillations appear at 22.5, 10 and 3.5 years (Figs. 7c, e and f). Correlation coefficients between the observed and reconstructed oscillations indicate large similarities in cycles around 23–25, 8.7–8.9 and 3–5 years (Fig. 7). However, the associated variance is relatively low at most of these oscillations with exception of the 25.1 and 22.5 year cycles that explain 11.5% and 27.2% of the total variance for the reconstructed and observed streamflow records, respectively.

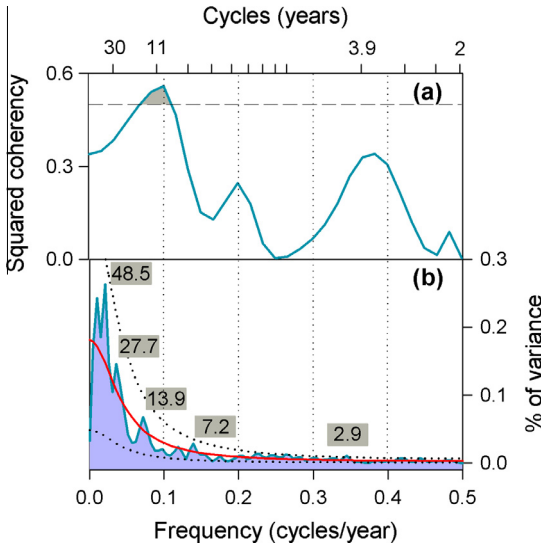

Fig. 6. (a) Coherency spectrum of instrumental and reconstructed Río Bermejo streamflow, estimated over the 1941–2001 common period. Dashed line indicate the 0.05 confidence level. (b) Blackman-Tuckey spectral density of the reconstructed (1680–2001) Río Bermejo streamflow. Dotted lines represent the 95% confidence limits based on a first-order Markov null continuum model and the solid line is the red noise band (the last peak -at 2.9 yr- is statistically highly significant).

4.2. Large-scale climatic influences

Spatial correlation patterns between Río Bermejo streamflow in summer (December–March) and meteorological variables were determined across South America and adjacent regions (20°N–60°S, 20°–100°W) for the wet 1975–2005 period in both instru-

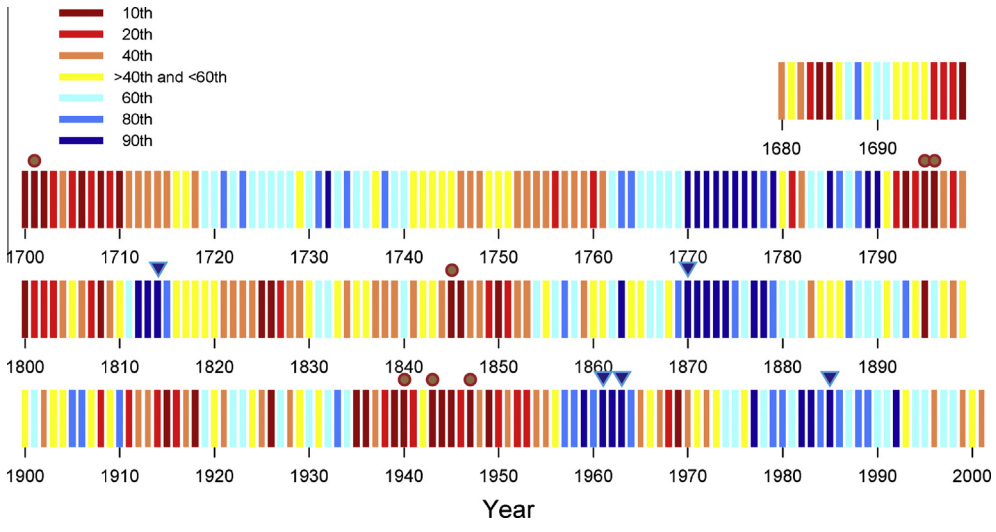

Fig. 5. Reconstructed Río Bermejo annual streamflow (1680–2001), categorized by percentiles. Values are shaded according to percentiles of flow. Years marked with *triangles* are the highest 98% of flow, while years with *circles* represent the lowest 2% of flow. Three of the wettest and driest events ever recorded, occurred in the last sixty years. (Modified from Meko and Woodhouse, 2011).

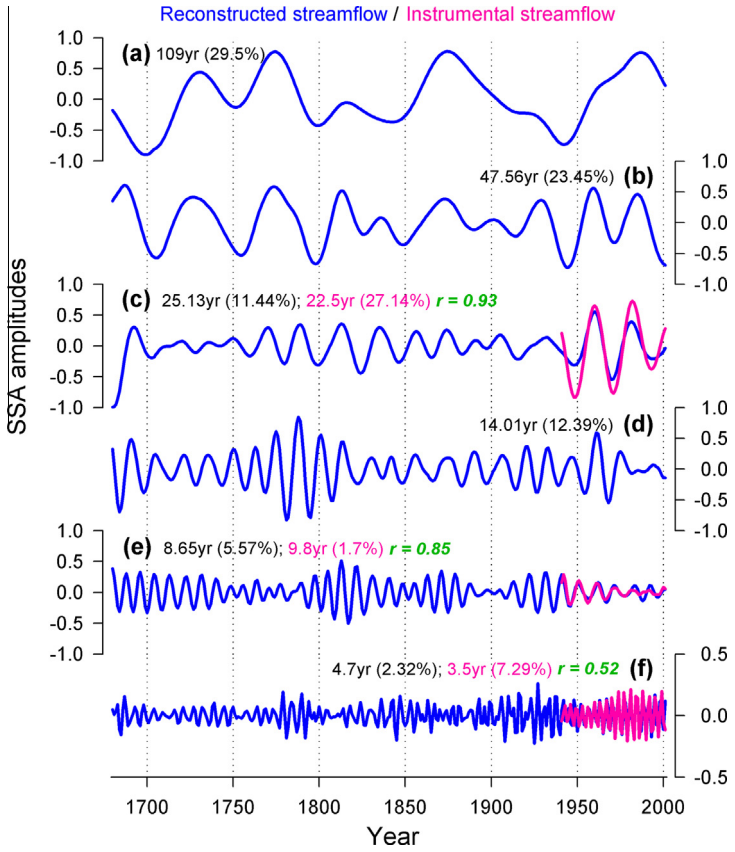

Fig. 7. Río Bermejo streamflow reconstruction most significant oscillation modes estimated by singular spectrum analysis (SSA). For comparison, main modes in actual streamflows are shown in pink lines. The frequencies for each SSA are indicated in years (yr), and the percentage of explained variance by each frequency shown in parentheses. When corresponding, correlation coefficients between the instrumental and reconstructed oscillations are indicated.

mental and reconstructed records (Fig. 8). Streamflow records show significant correlations with OLR mostly over the south/eastern Bolivia and northern Argentina, as well as southern Amazonia (Fig. 8a). The correlation coefficients between the reconstructed streamflow and gridded precipitation data for the summer season (Fig. 8b) is also coherent with OLR correlation, showing highest

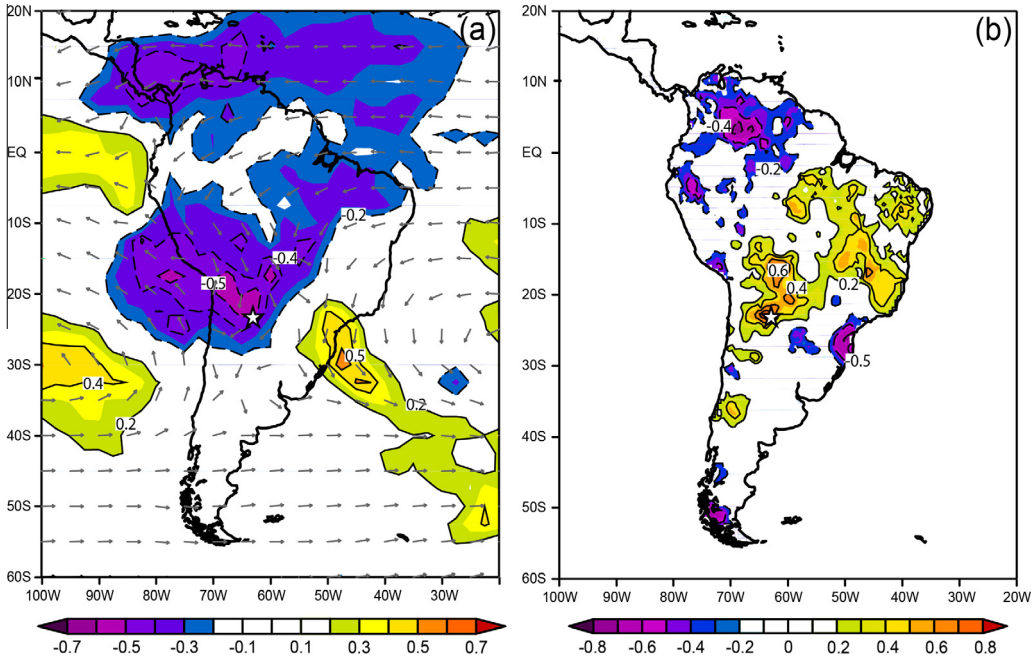

Fig. 8. Spatial correlation patterns during the 1975–2005 interval between December–March (a) instrumental Bermejo streamflow and outgoing longwave radiation (OLR); mean (1975–2005) 850 hPa wind vector is shown as arrows, and (b) Río Bermejo reconstructed streamflow with surface precipitation. Positive (negative) contour correlations are shown in *solid* (*dashed*) *lines*; zero contours are omitted. *Star symbol* approximate Río Bermejo study site.

values at eastern Bolivia, northern Paraguay and northwestern Argentina, as well as southern Amazonia. In both spatial patterns, a well-represented common feature is given by the inverse relationships over the SACZ region in south-eastern South America (SESA), both at high (200 hPa) and surface levels.

5. Discussion

The abundance and diversity of natural resources in the subtropical Bermejo basin contrasts with high social and environmental vulnerabilities due to land degradation and accelerated loss of renewable resources. Recently, droughts and floods have exacerbated the deterioration of native forests and cultivated areas. In this contribution, we reconstructed multi-century Río Bermejo streamflow variability based on tree-ring chronologies from subtropical regions in South America. The May–October dry season streamflow reconstruction of Río Bermejo covers the interval 1680–2001, utilizes an effective method to increase the number of tree-ring chronologies used as predictors, and captures the large-scale spatial patterns of subtropical hydrological variability.

The *J. australis*, *S. lorentzii* and *C. lilloi* composite chronologies developed in this study are robust, well replicated and capture larger regional climatic signals than individual tree-ring chronologies. This represents a major advance in relation to previous work in subtropical dendrochronology in South America, where past climate variations were mostly inferred from single chronologies (Villalba et al., 1992, 1998). Although the use of composite chronologies reduces the number of potential predictors in climate reconstructions, it improves the quality of the records and facilitates the capture of common climatic signals at a regional spatial scale (Villalba et al., 2012). Diverse relationships between instrumental streamflows and chronologies reflects the large variability in tree-growth responses to climate in the very heterogeneous environments of subtropical northwestern Argentina. The chronologies used as predictors for the reconstruction are located across different environments in upper Río Bermejo basin and integrate the regional variability of rainfall in this sector of the basin, which represents the primary source of water for Río Bermejo. The evaluation of the nested models indicates less reliability at both extremes of the reconstruction (1680–1778, 1992–2001) in comparison with the rest of the reconstruction due to the reduction in the number of predictor chronologies. In Model 4 (used to extend the reconstruction to 1680), the lower quality of the reconstruction could also be related to some differences in tree responses to climate for the RHN composite chronology (CC5). These composite chronology sites are located at high, cold and wet environments and show significant strong negative responses to instrumental flow variations suggesting a larger sensitivity of tree growth to temperature than precipitation during the growing season. However, there is a strong negative relationship between regional precipitation and temperature. The wettest years are generally the coldest, which possibly explains the relationship between the chronologies sensitive to temperature and river flow. The model 5 (1821–2001), used to reconstruct the last 10 years in Río Bermejo streamflow, better captures dry-to-relatively mild than wet years. During extreme wet periods (as indicated by the instrumental record from 1996), tree requirements for moisture become saturated and the magnitude of these very humid events are underestimated. Other authors (e.g. Masiokas et al., 2012) have identified such limitations in hydroclimatic reconstructions. In spite of these limitations, the tree-ring based reconstruction of Río Bermejo provides for the first time the opportunity to investigate interannual to multidecadal hydrological changes in subtropical areas of South America. It also allows the assessment of the severity of extreme events over a substantially larger context than those provides by the instrumental record.

Since regression statistics showed better skill of our predictor (composite chronologies) with the streamflow during the winter-spring season, we decided to reconstruct the streamflow during the dry season, concurrent with the lower Río Bermejo flows. Trees at highly seasonal-climatic environments such as northwestern Argentina appear to be more sensitive to climate during the season with the largest water deficit along the year. In the subtropics of South America, warmest temperatures occurs in spring (September to November) at the end of the dry season and preceding the onset of the summer rainy season. These high temperatures intensify the winter-early spring seasonal drought increasing evapotranspiration and heightening the water deficit. In consequence, the water shortage in soil at the end of the dry season is the major limitation for tree growth at regional scale. Abundant precipitations during the following summer months replenish the soil water capacity and provide water in larger amounts than those required by trees. Therefore, tree growth is more sensitive to soil water content in late winter-spring than during the pluvial summer months. Similar larger tree sensitivity to dry season conditions have also been reported for conifers in the temperate northern Patagonia, where precipitation is highly concentrated during the fall-winter months (Lara et al., 2008).

During the most replicated portion (1821–1992) of Río Bermejo reconstruction, the composite chronologies explain 50% of May–October (dry season) streamflow variability. Nevertheless, our reconstruction is significant correlated ($r \cong 0.51$) with instrumental summer-fall (January–April) streamflow during the wet season (Fig. 4). Interannual variations for dry and wet season streamflows over northwestern Argentina are significantly correlated ($r = 0.642$, $P < 0.01$) over the period 1941–2012 (72 years). These observations are consistent with recent analyses of the interdecadal modes of variability of monsoon precipitation over South America by Grimm and Saboia (2015). These authors found significant relationships between interdecadal variability in spring and summer, suggesting not just local but also remote influences on climate variations across South America. Indeed, Grimm and Saboia (2015) documented that the summer second mode and its related spring fourth mode of monsoon precipitation over South America, which affect the core monsoon region in central Brazil and northwestern Argentina (our study region), show similar factor loadings, indicating persistence of climatic anomalies from spring to summer season. In consequence, although our reconstruction performs better over the dry season, it also contains important information on past streamflow variations during the wet summer season.

There are no other streamflow reconstructions in tropical/subtropical South America to compare with our reconstruction. Nevertheless, the reconstruction statistics are comparable to other streamflow reconstructions using different species in different regions [e.g. D'Arrigo et al. (2011) for Indonesia; Mundo et al. (2012) for northern Patagonia]. Additional collections of subtropical species across the region should focus on expanding the tree-ring records for extending temporal coverage to strengthen the reconstruction during 17th and 21th centuries.

The reconstruction indicates that, in the last three centuries, there have been five very wet events that have exceeded the 98% of the discharge values (1814, 1870, 1961, 1963 and 1985), three of which are in the last 30 years (Fig. 5). Based on the instrumental series, years with flows above the 90th percentile were 1961, 1977, 1981–82/84–85, 1988, 1996, 1999–2000 and 2004, with values larger than 780 m^3/s (the average flow from May to October is 536 m^3/s for 1941–2012 period). Similarly, seven very dry events below the 2% of flow were recorded whithin the reconstruction (1701, 1795, 1796, 1845, 1940, 1943 and 1947), three of which occurred during the 20th century. In the context of the past

300 years provided by the reconstruction, oscillations from wet to dry conditions have been observed throughout the last centuries (Fig. 3). However, the persistence of extreme events, both high and low flow years, have been more frequent in recent decades. Streamflow variability was below the long-term mean during 1900–1950, but significantly increased from 1960s to present. These results are consistent with hydrological variations in Laguna Mar Chiquita, located in the subtropical Pampas of Argentina. The record of lacustrine sediments for Laguna Mar Chiquita extends from 13.0 Ka to the present. Piovano et al. (2009), noted the occurrence of short-lived humid pulses during the second half of the 19th century (1850–1870) as well as peaks at ~1770. The large wet climate anomaly starting in 1976 is also well documented in the limnological record. The comparison of the wetter intervals in the lacustrine and tree rings records indicates a common climate signal for the subtropical region of Argentina, under the influence of SASM.

The Blackman–Tukey and singular spectral analyses of the river reconstruction indicate that one of the main modes in spectral variability is dominated by a 25–27.7 year cycle, which explains 11.5% of of the total variance. This oscillatory mode is also present in the instrumental streamflow record explaining ~27% of Río Bermejo variance from 1941–2012. This periodicity has been detected in various instrumental records in tropical/subtropical South America and is consistent with variations in the Pacific Decadal Oscillation [PDO, a low-frequency (20–30 yr) oceanic oscillation of the North Pacific SSTs; Mantua et al., 1997]. A well-known transition in the PDO, occurred in 1975–1977 and is associated with the onset of a positive precipitation trend in southern Amazonia since early 1970s (Agosta and Compagnucci, 2008). It is embedded in a 26 year cycle, suggesting a decadal-scale variability in precipitation for southern Amazonia and the adjacent subtropics in South America (Marengo, 2004). These observations are consistent with observations by Jacques-Coper and Garreaud (2014) who analyzed the mid-1970s climate shift over South America. After the 1970s, they recorded dry anomalies in annual precipitation in tropical South America north of 10°S and wet anomalies to the south, including the Río Bermejo basin in the subtropics, associated to the concurrent PDO change to the warm phase. The observed change in the precipitation pattern over southern Amazonia and western Argentina around the mid-1970s has been related to the intensification of the meridional low-level jet from the humid lowlands of Brazil and Bolivia to central South America, leading to more moisture advection after the 1970 shift (Compagnucci et al., 2002). Transient moisture flux from Amazonia to the south is also important for the maintenance of SACZ, and its establishment is distinctive of the mature monsoon across South America (Vera et al., 2006). Power- and singular-spectral analyses from Río Bermejo streamflow reconstruction indicate, in addition to the 27 year cycle, the presence of a low-frequency oscillation at periods of approximately 14 years, which explains around 12.4% of total streamflow variance (Figs. 6 and 7). Robertson and Mechoso (2000) have observed interdecadal variability around 15 years in the SACZ activity, consistent with the second largest low-frequency oscillatory mode in Río Bermejo reconstruction. The climate association between the SALLJ and the SACZ dipole-like pattern has been identified in various timescales (Marengo et al., 2012); one phase of the dipole is characterized by enhancement of the SACZ and a suppression of the convection to the south, and viceversa. The strengthening of the SALLJ and the associated transports of massive amounts of moisture from the Amazon basin into the subtropics is accompanied by a weaker SACZ.

Although the Río Bermejo reconstruction is centered in the dry season of the year (May–October), it also captures some atmospheric components of the monsoon system of South America. The spatial correlation map between outgoing longwave radiation (OLR) and instrumental records of Río Bermejo (Fig. 8a), show areas of great convective activity associated with the mature phase of SASM (December–March) and intensified winds at 850 hPa east of the Andes related to the low-level flow (SALLJ) from southwestern Amazonia. Spatial correlations between the Río Bermejo streamflow reconstruction and gridded summer precipitation (Fig. 8b) over South America, showing precipitation regions between 10° and 30°S east of the Andes, are consistent to convection over the Amazon and intensified SALLJ activity. In consequence, the air masses that feed the moisture flow over the subtropics east of the Andes are strongly linked to large-continental monsoonal circulation in summer. It is noteworthy that in both spatial patterns (Fig. 8a and b), positive correlations of precipitation and OLR over the Bermejo basin, contrast with opposite values over the SACZ region in southeastern South America (SESA), consistent with the previously described seesaw pattern between the SALLJ and the SACZ, documented in instrumental records (e.g. Marengo et al., 2012).

Knowledge of past high and low flow events and information on current streamflow behavior are important for water resource management in the Río Bermejo basin. Precipitation and hence streamflow are projected to increase in amount and variability in the subtropical montane regions of South America (Marengo et al., 2010) impacting river dynamics, with major implications for human activities and social vulnerability. The scarcity of studies describing the tropical climate variability based on instrumental records (e.g. Marengo, 2004; Jacques-Coper and Garreaud, 2014) emphasized for the region the need of long-term records for a comprehensive understanding of climate fluctuations in subtropical regions of South America. The streamflow reconstruction described in this paper provides, for the first time, a longer perspective for the study of the mechanisms of atmospheric circulation that connect tropical with subtropical regions in South America.

Acknowledgements

This research was supported by Consejo Nacional de Ciencia y Técnica (CONICET) doctoral fellowship, ANPCyT (PICTR2002-123 project) and by the Inter-American Institute for Global Change Research (IAI-CRN2047). The Subsecretaría de Recursos Hídricos de la Nación (Argentinean National Agency of Water Resources) provided hydrological records for gauging stations. We appreciate the support of David Meko (Laboratory of Tree-Ring Research, The University of Arizona) with the "leave-one-out" routine. Petr Stepanek provided the AnClim software for the calculation of power spectra (http://www.climahom.eu). We also utilized the RespoSum routine developed by Mariano Masiokas (IANIGLA, CCT-Mendoza).

Authors wish to acknowledge José Boninsegna, Duncan Christie, Mariano Morales and specially Ignacio Mundo for providing assistance with statistical analysis; Lidio López and Mariano Masiokas contributed greatly with software support. We thank two annonymous reviewers for their comments and suggestions.

Appendix A. Supplementary material

Supplementary data associated with this article can be found, in the online version, at http://dx.doi.org/10.1016/j.jhydrol.2015.04.004.

References

Agosta, E.A., Compagnucci, R.H., 2008. The 1976/77 austral summer climate transition effects on the atmospheric circulation and climate in southern South America. J. Clim. 21, 4365–4383.

Anchukaitis, K.J., Taylor, M.J., Leland, C., Pons, D., Martin-Fernandez, J., Castellanos, E., 2014. Tree-ring reconstructed dry season rainfall in Guatemala. Clim. Dyn. http://dx.doi.org/10.1007/s00382-014-2407-y.

Arnell, N., Liu, C., Compagnucci, R., da Cunha, L., Hanaki, K., Howe, C., Mailu, G., Shiklomanov, I., Stakhiv, E., 2001. Hydrology and water resources. In: McCarthy, J.J., Canziani, O.F., Leary, N.A., Dokken, D.J., White, K.S. (Eds.), Climate Change 2001: Impacts, Adaptation and Vulnerability. Contribution of Working Group II to the Third Assessment Report of the Intergovernmental Panel on Climate Change. Cambridge University Press, Cambridge, pp. 191–234.

Blasing, T.J., Solomon, A.M., Duvick, D.N., 1984. Response functions revisited. Tree-Ring Bull. 44, 1–15.

Boninsegna, J.A., Argollo, J., Aravena, J.C., Barichivich, J., Christie, D., Ferrero, M.E., Lara, A., LeQuesne, C., Luckman, B.H., Masiokas, M., Morales, M., Oliveira, J.M., Roig, F., Srur, A., Villalba, R., 2009. Dendroclimatological reconstructions in South America: a review. Palaeogeogr. Palaeocl. 281, 210–228.

Brea, J.D., Spalletti, P., 2010. Generación y transporte de sedimentos en la Cuenca Binacional del Río Bermejo. Caracterización y análisis de los procesos intervinientes. COBINABE, Buenos Aires.

Briffa, K.R., 1995. Interpreting high-resolution proxy climate data: the example of dendroclimatology. In: Von Storch, H., Navarra, A. (Eds.), Analysis of Climate Variability: Applications of Statistical Techniques. Springer, Berlin, pp. 77–94.

Brown, A.D., Chalukian, S.C., Malmierca, L.M., 1985. Estudio florístico-estructural de un sector de selva semidecidua del noroeste argentino. I. Composición florística, densidad y diversidad. Darwiniana 26, 27–41.

Cabrera, A.L., 1976. Enciclopedia Argentina de Agricultura y Jardinería. Acme S.A.C.I, Buenos Aires.

Camilloni, I., Barros, V., 2000. The Paraná river response to El Niño 1982–83 and 1997–98 events. J. Hydrometeor. 1, 412–430.

COBINABE, 2010. (Comisión Binacional para el Desarrollo de la Alta Cuenca del Río Bermejo y el Río Grande de Tarija. Memoria 1995–2010), first ed. Buenos Aires.

Cobos, D.R., Boninsegna, J.A., 1983. Fluctuations of some glaciers in the upper Atuel River basin, Mendoza, Argentina. Quat. S. Am. Antarct. Peninsula 1, 61–82.

Compagnucci, R.H., Agosta, E.A., Vargas, M.W., 2002. Climatic change and quasi-oscillations in central-west Argentina summer precipitation: main features and coherent behaviour with southern African region. Clim. Dyn. 18, 421–435.

Cook, E.R., Krusik, P., 2005. A tree-ring standardization program based on detrending and autoregresive time series modeling, with interactive graphics. Tree-Ring Laboratory Lamont Doherty Earth Observatory, Columbia University, New York.

Cook, E.R., Briffa, K.R., Jones, P.D., 1994. Sparial regression methods in dendroclimatology: a review and comparison of two techniques. Int. J. Climatol. 14, 379–402.

Cook, E.R., Meko, D.M., Stahle, D.W., Cleaveland, M.K., 1999. Drought reconstructions for the continental United States. J. Clim. 12, 1145–1162.

Cook, E.R., D'Arrigo, R., Mann, M., 2002. A well-verified, multiproxy reconstruction of the winter North Atlantic Oscillation index since A.D. 1400. J. Clim. 15, 1754–1764.

Cook, E.R., Woodhouse, C.A., Eakin, C.M., Meko, D.M., Stahle, D.W., 2004. Long-term aridity changes in the western United States. Science 203, 1015–1018.

Cooley, W.W., Lohnes, P.R., 1971. Multivariate Data Analysis. Wiley, New York.

D'Arrigo, R.D., Abram, N., Ummenhofer, C., Palmer, J., Mudelsee, M., 2011. Reconstructed streamflow for Citarium River, Java, Indonesia: linkages to tropical climate dynamics. Clim. Dynam. 36, 451–462.

Ferrero, M.E., 2011. Cambios en el crecimiento leñoso de las regiones subtropicales de América del Sur en relación con la variabilidad climática. PhD. Dissertation, Universidad Nacional de Córdoba, Córdoba, pp. 228.

Ferrero, M.E., Villalba, R., 2009. Potential of *Schinopsis lorentzii* for dendrochronological studies in subtropical dry Chaco forests of South America. Trees 23, 1275–1284.

Ferrero, M.E., Villalba, R., De Membiela, M., Ripalta, A., Delgado, S., Paolini, L., 2013. Tree-growth responses across environmental gradients in subtropical Argentinean forests. Plant Ecol. 214, 1321–1334.

Ferrero, M.E., Villalba, R., Rivera, S.M., 2014. An assessment of growth ring identification in subtropical forests from northwestern Argentina. Dendrochronologia 32, 113–119.

Flamenco, E.A., Villalba, R., Rodriguez, R., 2011. Historical reconstruction of flow in Northwest Argentina on dendrochronological records. J. Hydrol. Environ. 7, 123–130.

Fritts, H.C., 1976. Tree Rings and Climate. Academic Press, London.

Garreaud, R., Vuille, M., Compagnucci, R., Marengo, J., 2009. Present day South America climate. Palaegeogr. Palaeocl. 281, 180–195.

Gasparri, N.I., Grau, H.R., Gutiérrez Angonese, J., 2013. Linkages between soybean and neotropical deforestation: coupling and transient decoupling dynamics in a multi-decadal analysis. Glob. Environ. Change 23, 1605–1614.

Grau, H.R., Brown, A.D., 1995. Pattern of tree species diversity along latitudinal and altitudinal gradients in the Argentinean subtropical montane forests. Biodiversity and conservation of Neotropical montane forests. In: Proc. Symposium, New York Botanical Garden.

Grimm, A.M., Saboia, J.P.J., 2015. Interdecadal variability of the South American precipitation in the monsoon season. J. Clim. 28, 755–775.

Holmes, R.L., 1983. Computer-assisted quality control in tree rings dating and measurement. Tree-Ring Bull. 43, 69–75.

Holmes, R.L., Stockton, C.W., LaMarche, V.C., 1979. Extension of river flow records in Argentina from tree-ring chronologies. J. Am. Resour. Assoc. 15, 1081–1085.

IPCC, 2007. Working group II: impacts, adaptation and vulnerability. In: Parry, M.L., Canziani, O.F., Palutikof, J.P., van der Linden, P.J., Hanson, C.E. (Eds.), Fouth Assessment Report of the Intergovernmental Panel on Climate Change. Cambridge University Press, Cambridge.

Jacques-Coper, M., Garreaud, R., 2014. Characterization of the 1970s climate shift in South America. Int. J. Climatol, doi: 10.1002/joc.4120.

Jenkins, G.M., Watts, D.G., 1968. Spectral Analyses and Its Applications. Holden-Day, San Francisco.

Lara, A., Villalba, R., Urrutia, R., 2008. A 400-year tree-ring record of the Puelo River summer-fall streamflow in the Valdivian reinforest ecoregion. Chile. Clim. Change 86, 331–356.

Lara, A., Bahamondez, A., González-Reyes, A., Muñoz, A.A., Cuq, E., Ruiz-Gómez C., 2014. Reconstructing streamflow variations of the Baker River from tree-rings in Northern Patagonia since 1765. J. Hydrol., in press.

Liebmann, B., Smith, C.A., 1996. Description of a complete (interpolated) outgoing longwave radiation dataset. B. Am. Meteorol. Soc. 77, 1275–1277.

Mantua, N.J., Hare, S.R., Zhang, Y., Wallace, J.M., Francis, R.C., 1997. A Pacific decadal climate oscillation with impacts on salmon. B. Am. Meteorol. Soc. 78, 1069–1079.

Manzanal, M., Arrieta, J., 2000. Diagnóstico socioeconómico del sector argentino de la cuenca del Río Bermejo. Programa estratégico de acción (PEA-Bermejo), OEA, Buenos Aires.

Marengo, J.A., 2004. Interdecadal variability and trends of rainfall across the Amazon basin. Theor. Appl. Climatol. 78, 79-76.

Marengo, J.A., Ambrizzi, T., da Rocha, R.P., Alves, L.M., Cuadra, S.V., Valverde, M.C., Torres, R.R., Santos, D.C., Ferraz, S.E.T., 2010. Future change of climate un South America in the late twenty-first century: intercomparison of scenarios from three regional climate models. Clim. Dyn. 35, 1089–1113.

Marengo, J.A., Liebmann, B., Grimm, A.M., Misra, V., Silva Dias, P.L., Cavalcanti, I.F.A., Carvalho, L.M.V., Berbery, E.H., Ambrizzi, T., Vera, C.S., Saulo, A.C., Nogues-Paegle, J., Zipser, E., Seth, A., Alves, L.M., 2012. Recent developments of the South American monsoon system. Int. J. Climatol. 32, 1–21.

Masiokas, M.H., Villalba, R., Christie, D.A., Betman, E., Luckman, B.H., Le Quesne, C., Prieto, M.R., Mauget, S., 2012. Snowpack variations since AD1150 in the Andes of Chile and Argentina (30°–37° S) inferred from rainfall, tree-ring and documentary records. J. Geophys. Res. 117, D05112.

Masiokas, M.H., Villalba, R., Luckman, B.H., Montaña, E., Betman, D., Christie, D., Le Quesne, C., Mauget, S., 2013. Recent and historic Andean snowpack and streamflow variations and vulnerability to water shortages in central-western Argentina. In: Pielke, R.A. (Ed.), Climate Vulnerability: Understanding and Addressing Threats to Essential Resources. Elsevier, Academic Press, China, pp. 213–227.

Meko, D., 1997. Dendroclimatic reconstruction with time varying predictor subsets of tree indices. J. Climate 10, 687–696.

Meko, D.M., Woodhouse, C.A., 2011. Application of streamflow reconstruction to water resources management. In: Hughes, M.K., Swetnam, T.W., Diaz, H.F. (Eds.), Dendroclimatology Development in Paleoenvironmental Research 11. Springer, pp. 231–261.

Messerli, B., Viviroli, D., Weingartner, R., 2004. Mountains of the world: vulnerable water towers for the 21st century. AMBIO Special Report 13, 29–34.

Michaelsen, J., 1987. Cross-validation in statistical climate forecast models. J. Clim. Appl. Meterorol. 26, 1589–1600.

Mitchell, J.M., Dzerdseevskii, B., Flohn, H., Hofmeyr, W.L., Lamb, H.H., Rao, K.N., Wallen, C.C., 1966. Climatic Change. World Meteorological Organization, Geneva.

Mundo, I.A., Masiokas, M.H., Villalba, R., Morales, M.S., Neukom, R., Le Quesne, C., Urrutia, R.B., Lara, A., 2012. Multi-century tree-ring based reconstruction of the Neuquén River streamflow, northern Patagonia, Argentina. Clim. Past 8, 815–829.

Muñoz, A.A., 2012. Variabilidad multicentenial del crecimiento arbóreo y reconstrucciones de caudales en la transición climática templada mediterránea en Chile. PhD. Dissertation, Universidad Austral de Chile, Valdivia, pp. 109.

Organization of American States (OAS), 2005. Water Project Series, Number 1-October (<www.oas.org>).

Osborn, T.J., Briffa, K.B., Jones, P.D., 1997. Adjusting variance for sample size in tree-ring chronologies and other regional mean timeseries. Dendrochronologia 15, 9–99.

Paegle, J.N., Mo, K.C., 2002. Linkages between summer rainfall variability over South America and sea surface temperature anomalies. J. Clim. 15, 1389–1407.

Pedrozo, F., Bonetto, C., 1987. Nitrogen and phosphorus transport in the Bermejo River (South America). Rev. Hydrobiol. Trop. 20, 91–99.

Piovano, E.L., Ariztegui, D., Córdoba, F., Cioccale, M., Sylvestre, F., 2009. Hydrological variability in South America below the Tropic of Capricorn (Pampas and Patagonia, Argentina) during the last 13.0 Ka. In: Vimeux, F., Sylvestre, F., Khodri, M. (Eds.), Past Climate Variability in South America and Sorrounding Regions, Development in Paleoenvironmental Research, vol. 14. Springer, pp. 323–351.

Rafaelli, S.G., Montgomery, D.R., Greenberg, H.M., 2001. A comparison of thematic mapping of erosional intensity to GIS-driven process models in an Andean drainage basin. J. Hydrol. 244, 33–42.

Robertson, A.W., Mechoso, C.R., 2000. Interannual and interdecadal variability of the South Atlantic convergence zone. Mon. Weather Rev. 128, 2947–2957.

Saulo, C.E., Seluchi, M.E., Nicolini, M., 2004. A case study of a Chaco Low-Level Jet event. Mon. Weather Rev. 132, 2669–2683.

Schöngart, J., Junk, W., Piedade, M., Ayre, J., Hüttermann, A., Worbes, M., 2004. Teleconnection between tree growth in the Amazonian floodplains and the El Niño-Southern Oscillation effect. Glob. Change Biol. 10, 683–692.
Spichiger, R., Palese, R., Chautems, A., Ramella, L., 1995. Origin, affinities and diversity hot spots of the Paraguayan dendroflora. Candollea 50, 515–537.
Urrutia, R.B., Lara, A., Villalba, R., Christie, D.A., Le Quesne, C., Cuq, A., 2011. Multicentury tree-ring reconstruction of annual streamflow for the Maule River watershed in south central Chile. Water Resour. Res. 47, W06527.
Vautard, R., Ghil, M., 1989. Singular spectrum analysis in nonlinear dynamics, with applications to paleoclimate time series. Physica D 32, 395–424.
Vera, C., Higgins, W., Amador, J., Ambrizzi, T., Garreaud, R., Gochis, D., Gutzler, D., Lettenmaier, D., Marengo, J., Mechoso, C.R., Nogues-Paegle, J., Silva Dias, P.L., Zhang, C., 2006. Towards a unified view of the American monsoon systems. J. Clim. 19, 4977–5000.
Villalba, R., Boninsegna, J.A., Ripalta, A., 1987. Climate, site conditions and tree-growth in subtropical north-western Argentina. Can. J. For. Res. 17, 1527–1544.
Villalba, R., Holmes, R.L., Boninsegna, J.A., 1992. Spatial patterns of climate and tree growth variations in subtropical northwestern Argentina. J. Biogeogr. 19, 631–649.
Villalba, R., Grau, H.R., Boninsegna, J.A., Jacoby, G.C., Ripalta, A., 1998. Tree-ring evidence for long-term precipitation changes in subtropical South America. Int. J. Climatol. 18, 1463–1478.
Villalba, R., Lara, A., Masiokas, M.H., Urrutia, R., Luckman, B.H., Marshal, G.J., Mundo, I.A., Christie, D.A., Cook, E.R., Neukom, R., Allem, K., Fenwick, P., Boninsegna, J.A., Srur, A.M., Morales, M.S., Araneo, D., Palmer, J.G., Coq, E., Aravena, J.C., Holz, A., LeQuesne, C., 2012. Unusual Southern Hemisphere tree growth patterns induced by changes in the Southern Annular Mode. Nat. Geosci. 5, 793–798.
Viviroli, D., Weingartner, R., Messerli, B., 2003. Assessing the hydrological significance of the world's mountains. Mt. Res. Dev. 23, 32–40.
Weisberg, S., 1985. Applied Linear Regression, second ed. John Wiley, New York.
Wigley, T.M., Briffa, K.R., Jones, P.D., 1984. On the average value of correlated time series with applications in dendroclimatology and hydrometeorology. J. Clim. Appl. Meteorol. 23, 201–213.
Woodhouse, C.A., Lukas, J.J., 2006. Multi-century tree-ring reconstructions of Colorado streamflow for water resource planning. Clim. Change 78, 293–315.